TWMS J. App. Eng. Math. V.3, N.1, 2013, pp. 75-86

ENERGY PRESERVING INTEGRATION OF BI-HAMILTONIAN PARTIAL DIFFERENTIAL EQUATIONS

B. KARASÖZEN[1], G. ŞİMŞEK[2] §

Abstract. The energy preserving average vector field (AVF) integrator is applied to evolutionary partial differential equations (PDEs) in bi-Hamiltonian form with nonconstant Poisson structures. Numerical results for the Korteweg de Vries (KdV) equation and for the Ito type coupled KdV equation confirm the long term preservation of the Hamiltonians and Casimir integrals, which is essential in simulating waves and solitons. Dispersive properties of the AVF integrator are investigated for the linearized equations to examine the nonlinear dynamics after discreization.

Keywords: Energy preservation, bi-Hamiltonian systems, Poisson structure, KdV equation

AMS Subject Classification: 83-02, 99A00

1. Introduction

We consider integrable evolutionary equations in bi-Hamiltonian form ([16], Ch. 7.3) and [14, 17]:

$$\frac{\partial u}{\partial t} = \mathcal{J}_1 \frac{\delta \mathcal{H}_2}{\delta u} = \mathcal{J}_2 \frac{\delta \mathcal{H}_1}{\delta u} \tag{1}$$

in the domain $\Omega = (x,t) \in \mathbb{R} \times \mathbb{R}$, with x and t denoting space and time variables, respectively. Here, $\mathcal{J}_1$ and $\mathcal{J}_2$ are the skew-adjoint Hamiltonian operators which may depend on the solution $u(x,t)$ and its partial derivatives with respect to the spatial variable x. The variational derivative is given by

$$\frac{\delta \mathcal{H}}{\delta u} = \frac{\partial \mathcal{H}}{\partial u} - \partial_x \left(\frac{\partial \mathcal{H}}{\partial u_x} \right) + \partial_x^2 \left(\frac{\partial \mathcal{H}}{\partial u_{xx}} \right) - \cdots .$$

Many PDEs like the KdV equation, nonlinear Schrödinger equation, sine-Gordon equation are also represented in form of noncanonical Hamiltonian or Poisson systems with nonconstant skew-adjoint Hamiltonian operators, i.e. skew-adjoint Hamiltonian operators $\mathcal{J}_1$ and $\mathcal{J}_2$ are constant in (1), [14, 16, 17]. Symplectic or multisymplectic integrators do not preserve the nonconstant symplectic or Poisson structures [12]. There exist geometric integrators which preserve the Poisson structure for certain equations. For example, the symplectic Euler method and partitioned Lobatto IIIA-IIIB methods preserve the

[1] Department of Mathematics and Institute of Applied Mathematics, Middle East Technical University, 06800 Ankara, Turkey,
e-mail: bulent@metu.edu.tr

[2] Multiscale Engineering Fluid Dynamics, Department of Mechanical Engineering, Eindhoven University of Technology, P.O. Box 513, 5600 MB Eindhoven, The Netherlands,
e-mail: g.simsek@tue.nl

§ Manuscript received January 04, 2013.

Poisson structure of the Volterra lattice equation [9]. The nonconstant structure can be transformed to the constant one by the Darboux transformation or by using generating functions. However, explicit construction of the transformations is difficult, in practice.

Because there exist no general symplectic or multi-symplectic integrator for the bi-Hamiltonian systems with nonconstant structure in (1), one can look for energy preserving integrators. Conservation of the energy and other integrals of PDEs play an important role besides the preservation of the symplectic and multisymplectic structures, especially in the simulation of solitons. Numerical integrators, which preserve the Hamiltonian and other conserved quantities were developed before the geometric integrators emerged, but they have forgotten lately. In recent years, several energy or integral preserving methods were developed for ODEs and PDEs by using discrete gradients and discrete variational derivatives [5, 18]. After a suitable spatial discretization of the skew-adjoint operators and Hamiltonians in (1), the following finite dimensional Hamiltonian system is obtained:

$$\dot{\mathbf{u}} = J(\mathbf{u})\nabla H(\mathbf{u}), \quad \mathbf{u} \in \mathbb{R}^N. \tag{2}$$

Here, $J(\mathbf{u})$ is the $N \times N$ skew-symmetric structure matrix corresponding to the discretization of the skew adjoint operator $\mathcal{J}(u)$, and the operator ∇ is the standard gradient, which replaces the variational derivative.

In this paper, we apply the energy preserving average vector field (AVF) method [6]

$$\frac{\mathbf{u}^{n+1} - \mathbf{u}^n}{\Delta t} = J\left(\frac{\mathbf{u}^n + \mathbf{u}^{n+1}}{2}\right) \int_0^1 \nabla H(\mathbf{u}^n + \tau(\mathbf{u}^{n+1} - u^n))d\tau, \tag{3}$$

to KdV equation and to Ito's system in the bi-Hamiltonian form (1). It represents an extension of the implicit mid-point rule and an extension of averaged vector field integrators for canonical Hamiltonian systems [10] . Higher order AVF methods are constructed as collocation methods, and they are interpreted as Runge-Kutta methods with continuous stages for canonical and noncanonical Hamiltonian systems [6, 10]. The AVF method (3) is second order convergent in time. The spatial derivatives of the skew-adjoint operators and the Hamiltonians are discretized by central differences, second-order convergence is also retained in space. The AVF integrator (4) is symmetric and conjugate to a Poisson integrator, i.e., the quadratic Casimir functions are preserved exactly [6]. AVF methods require accurate computation of the integrals. The Hamiltonians of many PDEs are polynomial, so that the integrals in the AVF method are computed exactly at the beginning of the integration, and the computational complexity of the AVF method is comparable with the implicit symplectic Runge–Kutta methods. The numerical results confirm the excellent long-term preservation of the energy (Hamiltonian) and the integrals of the underlying equations. The soliton solutions obtained by the energy preserving AVF integrator show a very similar behavior, to those in the literature obtained by other symplectic and multi-symplectic methods. This indicates, that energy preservation provides long term accurate solutions like the geometric integrators.

The paper is organized as follows. In the next section, the formulation of the AVF method for the KdV equations and Ito's system is given with some numerical experiments, illustrating the energy preservation in long term integration.

2. Average vector field integration of bi-Hamiltonian PDE's

In this section, we apply the AVF method (3) to the KdV equation and Ito's system in bi-Hamiltonian form (1). We consider periodic boundary conditions such that no additional boundary terms will appear after semidiscretization. For discretization of (1) in space, it is crucial to preserve the skew-adjoint structure of $\mathcal{J}_1$ and $\mathcal{J}_2$ to obtain the semidiscrete Hamiltonian ODE of the form (2). The first order derivatives are discretized by backward finite differences and the Hamiltonians are approximated by the rectangle rule. The discrete approximation of $u(j\Delta x, n\Delta t)$ is denoted by $\mathbf{u}^n = (u_1^n, \ldots, u_j^n, \ldots, u_N^n)^T$

2.1. **Korteweg de Vries equation.** The KdV equation

$$u_t = \alpha u u_x + \rho u_x + \nu u_{xxx} \tag{4}$$

with the periodic boundary conditions $u(-L,t) = u(L,t)$ is given in bi-Hamiltonian [16, 17]

$$\mathcal{J}_1 = D, \quad \mathcal{H}_2 = \int \left(\frac{\alpha}{6}u^3 + \frac{\rho}{2}u^2 - \frac{\nu}{2}u_x^2\right) dx, \tag{5a}$$

$$\mathcal{J}_2 = \frac{\alpha}{3}uD + \frac{\alpha}{3}Du + \rho D + \nu D^3, \quad \mathcal{H}_1 = \int \frac{1}{2}u^2 dx, \tag{5b}$$

where $D = \partial_x$ denotes the first-order derivative with respect to space.

The skew adjoint operator $\mathcal{J}_1 = D$ of the first Hamiltonian formulation (6a) is discretized using central differences $Du = \frac{u_{j+1}-u_{j-1}}{2\Delta x}$ and yields the skew-symmetric matrix J_1

$$J_1 = \frac{1}{2\Delta x}A, \quad \text{with} \quad A = \begin{pmatrix} 0 & 1 & & & -1 \\ -1 & 0 & 1 & & \\ & \ddots & \ddots & \ddots & \\ & & -1 & 0 & 1 \\ 1 & & & -1 & 0 \end{pmatrix}, \tag{6}$$

where A is an $N \times N$ tridiagonal circulant matrix due to the periodic boundary conditions. The discrete form of the Hamiltonian $\mathcal{H}_2$ is given as

$$H_2 = \sum_{j=1}^{N} \left(\frac{\alpha}{6}u_j^3 + \frac{\rho}{2}u_j^2 - \frac{\nu}{2\Delta x^2}(u_{j+1}-u_j)^2\right)\Delta x.$$

After applying the AVF method (3) and by introducing the circulant matrix

$$B = \begin{pmatrix} -2 & 1 & & & 1 \\ 1 & -2 & 1 & & \\ & \ddots & \ddots & \ddots & \\ & & 1 & -2 & 1 \\ 1 & & & 1 & -2 \end{pmatrix},$$

we obtain the system of Hamiltonian ODEs consisting nonlinear and linear parts such as

$$\begin{aligned} \frac{\mathbf{u}^{n+1}-\mathbf{u}^n}{\Delta t} &= \frac{\alpha}{12\Delta x}A\left[(\mathbf{u}^n)^2 + \mathbf{u}^n\mathbf{u}^{n+1} + (\mathbf{u}^{n+1})^2\right] \\ &+ \frac{\rho}{4\Delta x}A\left(\mathbf{u}^n + \mathbf{u}^{n+1}\right) + \frac{\nu}{4\Delta x^3}A\cdot B\left(\mathbf{u}^n + \mathbf{u}^{n+1}\right). \end{aligned} \tag{7}$$

The second Hamiltonian formulation (6b) of the KdV equation is discretized similarly. The skew-adjoint operator $\mathcal{J}_2$ for the second Hamiltonian pair (5b) is more complicated

than $\mathcal{J}_1$, but the Hamiltonian $\mathcal{H}_1$ has a simpler form. The terms uD and Du are discretized together to preserve the self-adjointness of $\mathcal{J}_2$ as in [15] adapted to periodic boundary conditions

$$C(\mathbf{u}) = \begin{pmatrix} 0 & u_1+u_2 & & & -(u_1+u_N) \\ -(u_2+u_1) & \ddots & \ddots & & \\ & \ddots & \ddots & & u_{N-1}+u_N \\ u_1+u_N & & -(u_{N-1}+u_N) & & 0 \end{pmatrix}. \tag{8}$$

The circulant pentadiagonal matrix E

$$E = \begin{pmatrix} 0 & -2 & 1 & & -1 & 2 \\ 2 & \ddots & \ddots & \ddots & & -1 \\ -1 & \ddots & \ddots & \ddots & \ddots & \\ & \ddots & \ddots & \ddots & \ddots & 1 \\ 1 & & \ddots & \ddots & \ddots & -2 \\ -2 & 1 & & -1 & 2 & 0 \end{pmatrix} \tag{9}$$

corresponds to the discretization of D^3 by using central differences. Then, the discrete forms of $\mathcal{J}_2$ and $\mathcal{H}_1$ become

$$J_2 = \frac{\alpha}{6\Delta x}C(u) + \frac{\rho}{2\Delta x}A + \frac{\nu}{\Delta x^3}E, \quad H_1 = \frac{1}{2}\sum_{j=1}^{N} u_j^2 \Delta x.$$

Applying the AVF integrator (3) yields

$$\frac{\mathbf{u}^{n+1}-\mathbf{u}^n}{\Delta t} = \left(\frac{\alpha}{12\Delta x}(C(\mathbf{u}^n)+C(\mathbf{u}^{n+1})) + \frac{\rho}{2\Delta x}A + \frac{\nu}{\Delta x^3}E\right)\left(\frac{1}{2}\left(\mathbf{u}^{n+1}+\mathbf{u}^n\right)\right). \tag{10}$$

The fully discrete nonlinear equations (7) and (10) are solved by the Newton-Raphson method. As the circulant matrices have sparse structure and the nonlinear terms in the Jacobian appear in form of diagonal matrices, sparse routines of MATLAB are used to solve the linear equations to save storage and to decrease the computing time.

Example 1: We have taken the KdV equation in [1] with the parameters $\alpha = -1$, $\rho = 0$ and $\nu = -0.022^2$ and with the initial condition $u(x,0) = \cos(\pi x)$. We have used the same step sizes $\Delta x = 0.01$ and $\Delta t = 0.001$ as in [1] in the interval $x \in [0,2]$. The computations with AVF method are done with respect to the first Hamiltonian pair of KdV equation (5a). The error in the Hamiltonian or energy H_2 and the Casimir $I_2 = \frac{1}{2}\sum_{j=1}^{N} u_j^2 \Delta x$, are shown in Figure 1.

The error in the energy H_1 of the second Hamiltionian pair (5b) is preserved similar to the first Hamiltonian formulation (5a). The linear Hamiltonian H_2 is automatically preserved by the AVF method. Both are not shown here. Figure 2 shows solutions of the KdV equation using the AVF method (7), which shows a similar solutions as with those obtained by the symplectic and multisymplectic methods in [2] for the same time snapshots. Similar solutions are obtained for the second Hamiltonian formulation (10).

Example 2: We consider as a second example the KdV equation (4) with soliton solutions [22] under the initial condition $u(x,0) = \operatorname{sech}^2\left(\frac{x}{\sqrt{2}}\right)$ in the interval $x \in [-20,20]$. The parameters are $\alpha = -6$, $\rho = 0$ and $\nu = -1$. The mesh sizes in space and time are taken as $\Delta t = 0.02$ and $\Delta x = 40/150$. Energy error in the Hamiltonian and the Casimir

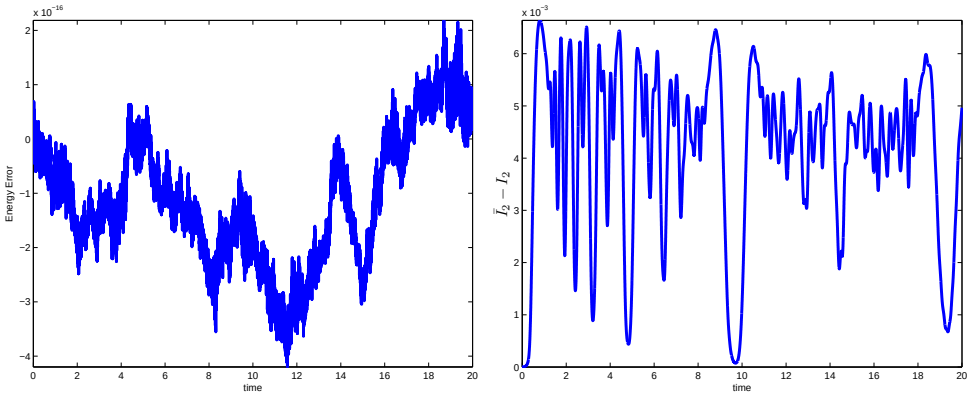

FIGURE 1. KdV equation: Error in the energy H_2 (left) and error in the Casimir I_2 (right) for the first bi-Hamiltonian formulation (5a).

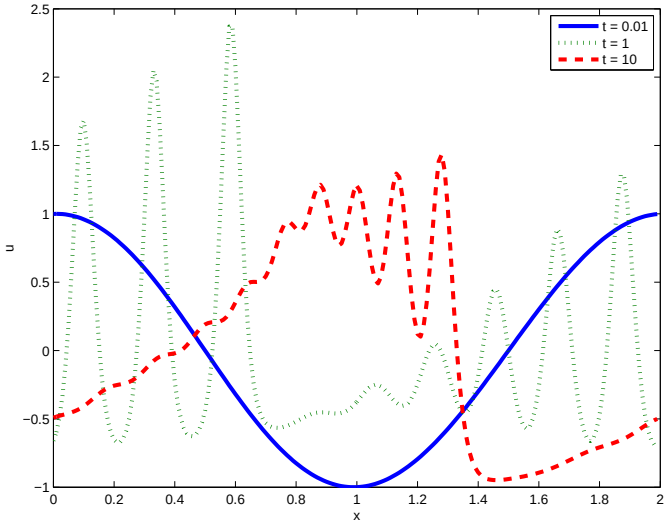

FIGURE 2. KdV equation: Solutions at various times $t = 0.01$, $t = 1$ and $t = 10$.

for the first formulation can be seen in Figure 3. Hamiltonian PDEs have distinguished integrals known as Casimirs $\mathcal{C}$, satisfying $J\frac{\delta \mathcal{C}}{\delta u} = 0$, i.e., their Poisson bracket vanishes for any function [16]. Among the infinitely many integrals of the KdV equation, the quadratic integral $\mathcal{I}_2 = \int \frac{1}{2}u^2 dx$ is a Casimir. AVF integrators [6, 10] preserve the quadratic invariants exactly.

Figure 3 shows that the energy is exactly preserved by the AVF method, whereas the Casimir is well preserved without any drift. The second formulation computations results are similar to those obtained from the first Hamiltonian formulation. The single soliton solution is displayed in Figure 4, which is the same as those given in [22] computed with the multisymplectic Preissmann scheme.

2.2. **Ito's System.** Ito's coupled KdV-type equations [11, 13, 21]

$$u_t + \alpha u u_x + \beta v v_x + \gamma u_{xxx} = 0, \quad v_t + \beta (uv)_x = 0, \tag{11}$$

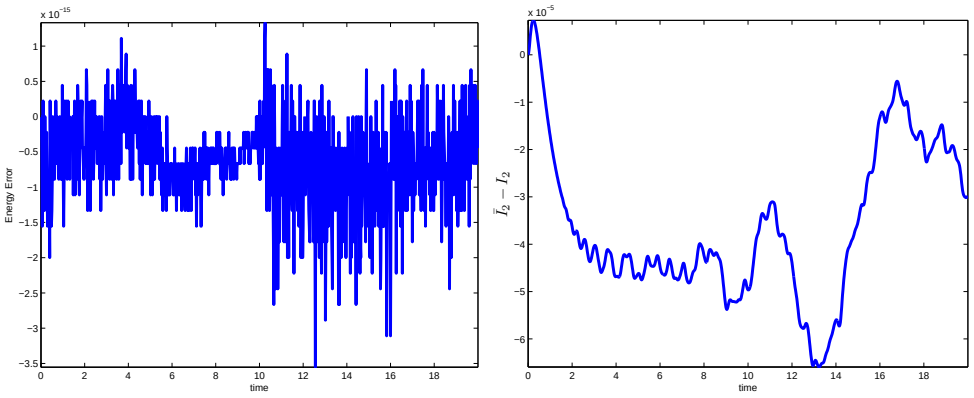

FIGURE 3. KdV equation: Energy error H_2 (left) and error in the Casimir I_2 (right).

are expressed as bi-Hamiltonian PDEs in [17] with $\alpha = -6$, $\beta = -2$, $\gamma = -1$ and

$$\mathcal{J}_1 = \begin{pmatrix} D & 0 \\ 0 & D \end{pmatrix}, \qquad \mathcal{H}_2 = \int \left(u^3 + uv^2 - \frac{u_x^2}{2} \right) dx, \tag{12a}$$

$$\mathcal{J}_2 = \begin{pmatrix} uD + Du + \frac{1}{2}D^3 & vD \\ Dv & 0 \end{pmatrix}, \quad \mathcal{H}_1 = \int \left(u^2 + v^2 \right) dx. \tag{12b}$$

Ito equation in bi-Hamiltonian forms above, is discretized similar to the KdV equation and solved by the AVF integrator.

Example 3: Ito's system is solved numerically by the AVF method with the initial conditions [21] $u(x,0) = \exp(-x^2)$, $\quad v(x,0) = \exp(-x^2)$, in the interval $x \in [-15, -15]$, by using $\Delta t = 0.001$ and $\Delta x = 30/160$. The Hamiltonian $\mathcal{H}_2$ and the quadratic first integral (Casimir) $I_2 = \int (\frac{2}{u} + v^2)$ of the Ito's system in the first bi-Hamiltonian form (12a) are preserved in Figure 5 up to the machine precision for the long time intervals. The

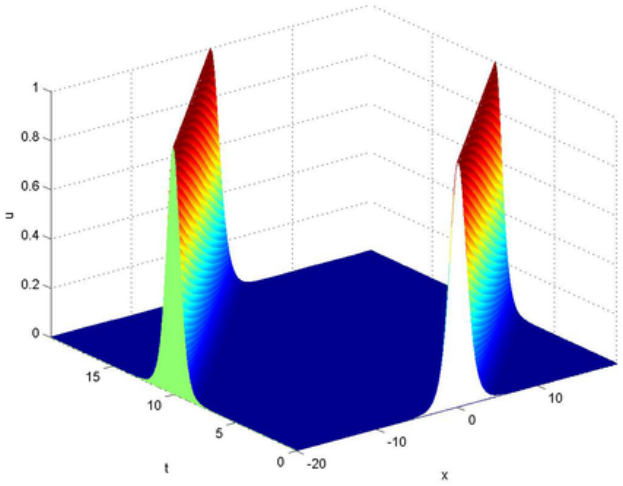

FIGURE 4. KdV equation: Single soliton solution

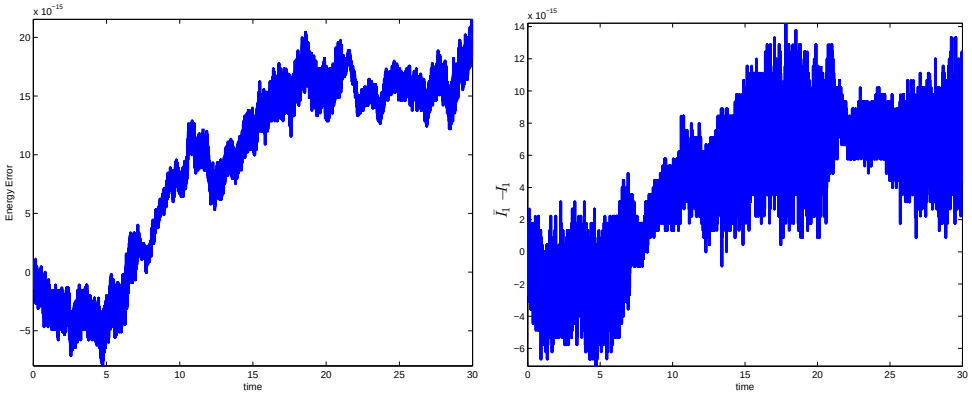

FIGURE 5. Ito's system: The error in the energy (left) and the in the conserved quantity $\mathcal{I}_1$ (right).

Hamiltonian $\mathcal{H}_1$ and the linear Casimir $\mathcal{I}_1 = \int(u+v)$, corresponding are almost exactly preserved and they are not shown here.

Solutions of the Ito's system for $t \in [0,2]$ and some instantaneous solutions at $t = 0, 1$ and 2 are shown in Figure 6. The first equation of (11) for u is a dispersive one, while there

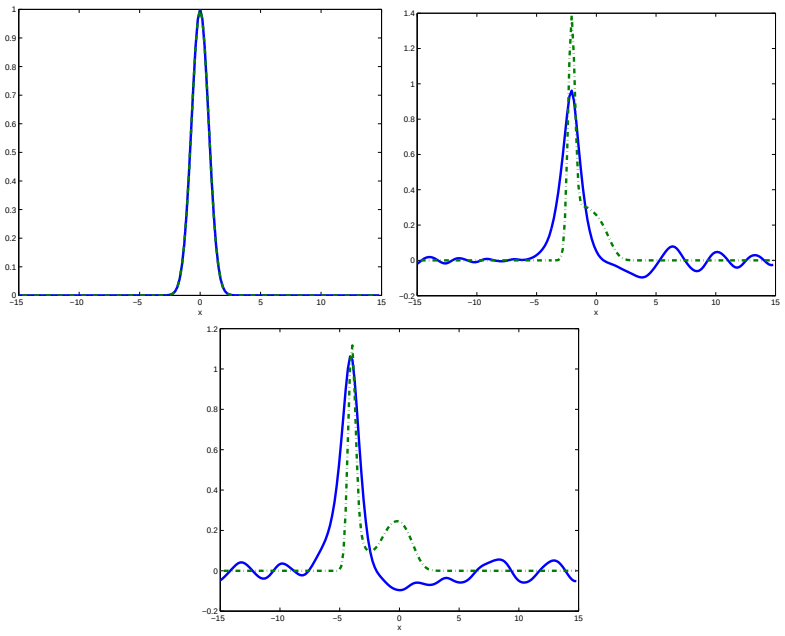

FIGURE 6. Solutions for u (solid) and v (dash dotted) at various time snapshots.

is no such dispersive term in the second equation for v. The existence of the dispersive wave $u(t)$ in the Ito's equation (11) is confirmed in Figure 6, whereas v is behaving like a shock wave, poised with some dispersion introduced by the AVF method. These results are similar to those in [21] where (11) is integrated by a local discontinuous Galerkin method.

The behavior of the numerical solutions of the Ito's system will be explained using the dispersion relation in the next section.

3. Dispersion relations

Nonlinear PDEs such as KdV equation (4) and Ito's equation (11) are dispersive, which means that the wave packets with different wave numbers travel with different velocities. The preservation of the energy in long time can alone not explain the accuracy of the solutions. The behavior of a nonlinear PDE can be determined by the dispersion relation in regions where linearized PDE is a valid approximation to the nonlinear PDE. A dispersion relation $\omega = \omega(k)$ of a constant coefficient linear evolution equation determines how time oscillations $e^{i\omega t}$ are linked to spatial oscillations e^{ikx} of a wave number k. Any linear constant coefficients PDE has a solution of the form

$$u(x,t) = \int_{\infty}^{\infty} A(k) e^{i(kx+\omega(k)t)} dk, \qquad i = \sqrt{-1}, \tag{13}$$

where ω is the frequency and k is the wave number. The dispersion relation $D(\omega, k) = 0$ is obtained by assuming that each wave $Ae^{i(kx+\omega t)}$ itself is a solution of the linear PDE.

Each wave travels with the phase velocity $\omega_p(k) = \omega/k$, characterizing the speed of the wave front. Dispersion occurs if the phase speed is not constant. The speed of the energy transport of the composite wave packet is characterized by the the group velocity $\omega'(k)$. The non-vanishing group velocity dispersion causes spatial spreading of the wave packet. Numerical errors in the dispersion relation and the group velocities can lead to the propagation of the numerical wave with different velocity and can destroy the qualitative feature of the solutions [19]. In numerical simulations, it is important to preserve the sign of the group velocity in order to avoid spurious solutions. Recently, dispersive properties of symplectic and multisymplectic integrators for the KdV equation is examined in [1, 2]. It was shown that the multisymplectic Preissman box scheme qualitatively preserves the dispersion relation of the KdV equation and any hyperbolic equation [1, 2]. These results were generalized for linear PDEs to cover general $s-$stage Gauss–Legendre–Runge–Kutta methods [8]. For the multisymplectic Preismann and box schemes there exists a diffeomorphism between the continuous and discrete dispersion relations, such that the sign of the group velocity is preserved for the KdV equation [1, 2, 4], for the sine-Gordon equation [19], for the "good" Boussinesq equation [3].

Linearization of the KdV equation (4) around the constant solution $\bar{u}$ gives [1, 2]

$$u_t = a u_x + \nu u_{xxx}, \tag{14}$$

where $a = \alpha\bar{u} + \rho$. The dispersion relation, phase and group velocities are

$$\omega = ak - \nu k^3, \tag{15}$$

$$\frac{\omega}{k} = a - \nu k^2, \qquad \frac{d\omega}{dk} = a - 3\nu k^2, \tag{16}$$

respectively. Similarly linearization of Ito's system (11) around constant solutions $\bar{u}$ and $\bar{v}$ results in

$$\begin{aligned} u_t &= u_{xxx} + 6\bar{u}u_x + 2\bar{v}v_x, \\ v_t &= 2\bar{v}u_x + 2\bar{u}v_x. \end{aligned} \tag{17}$$

Continuous dispersion relations and group velocities are given as

$$\omega_1(k) = -k^3 + (3b + ac)k, \qquad \omega_2(k) = \left(b + \frac{a}{c}\right) k, \tag{18}$$

$$\frac{d\omega_1}{dk} = -3k^2 + (3b + ac), \qquad \frac{d\omega_2}{dk} = \left(b + \frac{a}{c}\right), \tag{19}$$

where $a = 2\bar{v}$, $b = 2\bar{u}$, $c = \hat{v}/\hat{u}$. Since the phase velocity $\omega_2(k)$ is constant, for the linearized equation v is not a dispersive wave, whereas the solution u has the same form of

dispersion relation $\omega_1(k)$ as the linearized KdV equation (14) and, therefore, it is dispersive.

Numerical dispersion relations are obtained using the discrete version of the Fourier mode (13):

$$\tilde{u}_j^n = \hat{u}e^{i(jk\Delta x + n\omega\Delta t)} = \hat{u}e^{i(j\bar{k}+n\bar{\omega})}, \tag{20}$$

where $\bar{k} = k\Delta x$ and $\bar{\omega} = \omega\Delta t$, denote the numerical wavenumber and the numerical velocity respectively in the range $-\pi \le \bar{k}, \bar{\omega} \le \pi$.

3.1. **The KdV equation.** Application of the AVF method to the linearized KdV equation (14) yields

$$\frac{\mathbf{u}^{n+1}-\mathbf{u}^n}{\Delta t} = \frac{1}{4\Delta x}A\left[(a+\rho)(\mathbf{u}^{n+1}+\mathbf{u}^n) + \frac{\nu}{\Delta x^2}(\mathbf{u}^{n+1}+\mathbf{u}^n)\right]. \tag{21}$$

and, substituting (20) into (21) , we obtain the numerical dispersion relation

$$\tan\left(\frac{\bar{\omega}}{2}\right) - \nu\frac{\lambda}{\Delta x^2}\sin\bar{k}(\cos\bar{k}-1) - \frac{\lambda}{2}(a+\rho)\sin\bar{k} = 0, \tag{22}$$

where $\lambda = \frac{\Delta t}{\Delta x}$. Since the tangent function is invertible in the interval $[-\frac{\pi}{2}, \frac{\pi}{2}]$, the explicit form of the numerical dispersion relation becomes

$$\bar{\omega}(\bar{k}) = 2\arctan\left(\nu\frac{\lambda}{\Delta x^2}\sin\bar{k}(\cos\bar{k}-1) + \frac{\lambda}{2}(a+\rho)\sin\bar{k}\right). \tag{23}$$

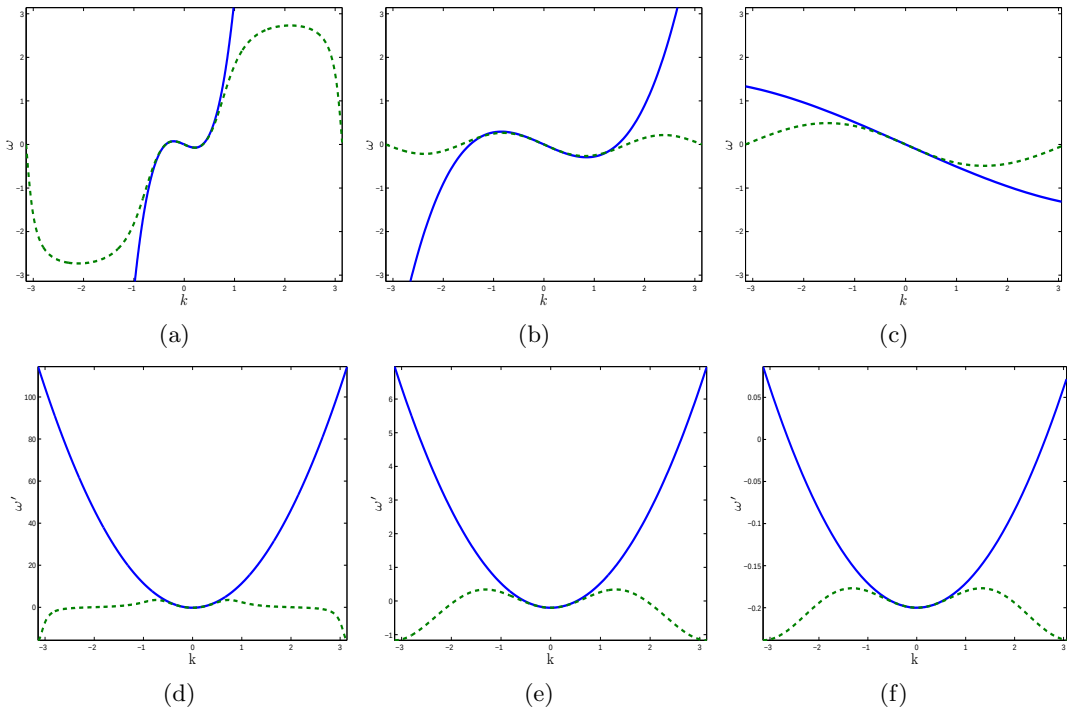

FIGURE 7. Dispersion curves (top) and group velocities (bottom) of the linearized exact (solid) and discretized (dotted) KdV for $\lambda = 0.2$. left $\Delta x = 0.005$, middle $\Delta x = 0.02$, right $\Delta x = 0.1$.

In Figure 7, the exact and numerical dispersion and group velocities of the linearized KDV equation are shown for the continuous ω, k and discrete $\bar{\omega}$, $\bar{k}$ frequencies and wavenumbers, respectively. The dispersion curves in Figures 7(a) and 7(b) are below the analytical dispersion curve for $\bar{k} > 0$. On the other hand, for $\Delta x = 0.1$, the dispersion curves for AVF make transitions from below to above the analytical curve at a value of the wave number $\bar{k}$ that depends on λ. In Figure 7a-c, for the continuous dispersion relations there is one frequency $\bar{\omega}$ corresponding to each wavenumber k, whereas there are multiple discrete wavenumbers $\bar{k}$ for each $\bar{\omega}$. This indicates that the AVF method introduces computational or parasitic modes. These are produced when the discretization yields different branches in the dispersion relation, which indicates that AVF approximates the solution for small wave numbers k well, but there are also modes giving poor approximations. When we compare the dispersion graphs in Figure 7a-c with the dispersion curves in [1, 2], we see that, the continuous and the numerical dispersion curves show similar behavior as for the implicit mid-point rule and non-compact schemes, whereas the multisymplectic box scheme preserves the dispersion relation for a long range of wave numbers k and spatial mesh size Δx.

In Figures 7d-f, the sign of the group velocity is preserved for long waves (small k), but it is not preserved for short waves by the AVF method for all Δx. This shows that the direction of the energy flow obtained from the AVF method may be different from the direction of the exact flow for short waves. The group velocity curves show that some numerical modes travel slower than the continuous ones and some numerical modes travel faster than the continuous ones as in [19].

3.2. **Ito's System.** After application of the AVF method to the linearized Ito system in Hamiltonian form

$$\mathcal{J} = \begin{pmatrix} 3bD + D^3 & aD \\ aD & bD \end{pmatrix}, \qquad \mathcal{H} = \int \frac{1}{2}(\tilde{\mathbf{u}}^2 + \tilde{\mathbf{v}}^2)dx.$$

we obtain

$$\begin{pmatrix} \vdots \\ \mathbf{u}_j^{n+1} - \mathbf{u}_j^n \\ \vdots \\ \mathbf{v}_j^{n+1} - \mathbf{v}_j^n \\ \vdots \end{pmatrix} = \frac{\Delta t}{2\Delta x} \begin{pmatrix} 3bA + \frac{\Delta t}{\Delta x^2} B & aA \\ aA & bA \end{pmatrix} \begin{pmatrix} \vdots \\ \frac{1}{2}\left(\mathbf{u}_j^{n+1} - \mathbf{u}_j^n\right) \\ \vdots \\ \frac{1}{2}\left(\mathbf{v}_j^{n+1} - \mathbf{v}_j^n\right) \\ \vdots \end{pmatrix}.$$

The corresponding numerical dispersion relations are given by

$$\begin{aligned} \bar{\omega}_1(\bar{k}) &= 2\arctan\left(\tfrac{\lambda}{\Delta x^2}\sin\bar{k}(\cos\bar{k} - 1) + (3b + ac)\,\tfrac{\lambda}{2}\sin\bar{k}\right), \\ \bar{\omega}_2(\bar{k}) &= 2\arctan\left(b + \tfrac{a}{c}\right)\tfrac{\lambda}{2}\sin\bar{k}. \end{aligned} \tag{24}$$

Figure 8 represents the dispersion and group velocity curves for both continuous dispersion relation (18) and the discrete dispersion relations (24). Dispersion properties of $u(t)$ (Figures 8a, 8c) are the same as the linearized KdV equation. The second component of Ito's system $v(t)$ is not a dispersive wave, but we see that the discretization introduces dispersion, so that only for a limited range of small wave numbers (Figures 8b, 8d) the numerical solution will be qualitatively correct.

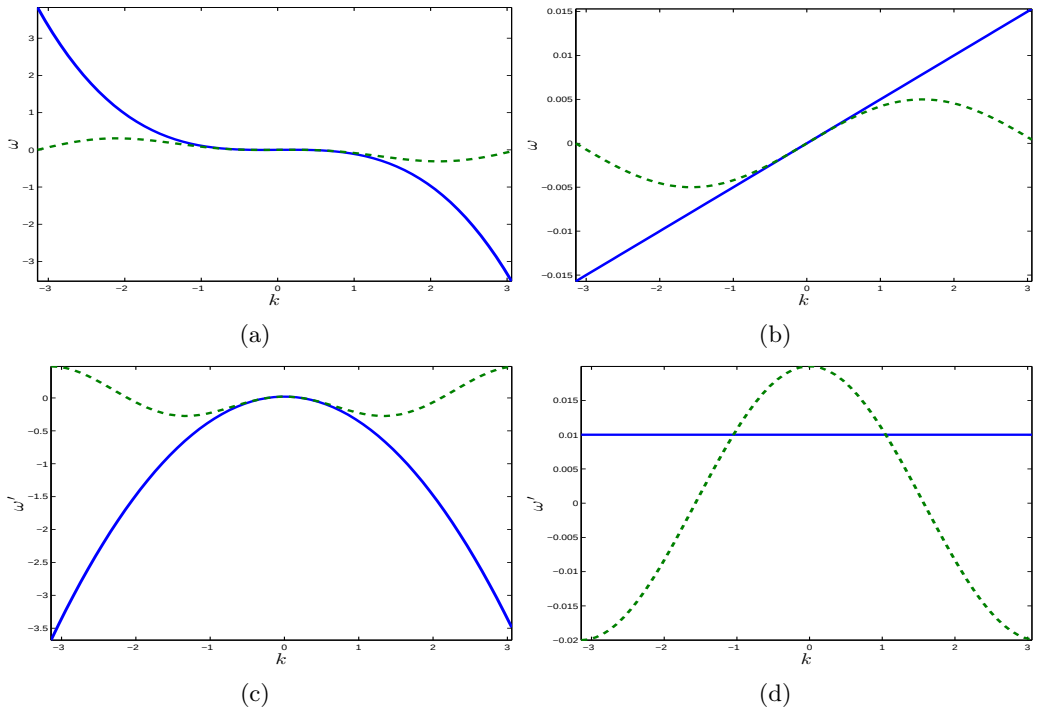

FIGURE 8. Dispersion curves (top) and group velocities (bottom) of the linearized Ito's system u (left) and v (right) for $\Delta t = 0.001$, $a = b = 1$ and $\lambda = 0.005$.

4. Conclusions

The numerical results confirm the excellent long-term preservation of the energy (Hamiltonian) and the integrals of the underlying equations. The numerically obtained soliton solutions show a very similar behavior, compared with those in the literature obtained by other methods. Dispersion analysis reveals that there does not exist such a diffemorphism between the continuous and discrete dispersion relations for the AVF method contrary to the mulyisymplectic integrators. Therefore for some wavenumber parasitic waves may exist.

Because the energy preserving methods are implicit as symplectic and multisymplectic integrators, the resulting nonlinear equations must be solved within the round-off error, to preserve symplecticity or the energy. This limits the applicability of these methods to large-scale systems. In these situations, either splitting can be used which are based on the splitting of the vector field in linear and nonlinear parts or linearly implicit methods which require the solution of precisely one linear system of equations in each time step [7].

References

[1] Ascher, U. M. and McLachlan, R. I., (2004), Multisymplectic box schemes and the Korteweg-de Vries equation, Appl. Numer. Math., 48, 255-269.

[2] Ascher, U. M., and McLachlan, R.I., (2005) On symplectic and multisymplectic schemes for the KdV equation. J. Sci. Comput., 25, 83-104.

[3] Aydın, A., and Karasözen, B., (2008), Symplectic and multisymplectic Lobatto methods for the "good" Boussinesq equation. J. Math. Phys., 49, 083509.

[4] Aydın, A., and Karasözen, B., (2010), Multisymplectic box schemes for the complex modified Korteweg-de Vries equation. J. Math. Phys., 51, 083511
[5] Celledoni, E., McLachlan, R. I., McLaren, D. I., Owren, B, Quispel, G. R. W. and Wright, W. M., (2009) Energy-preserving Runge-Kutta methods, M2AN Math. Model. Numer. Anal., 43, 649-645.
[6] Cohen, D. and Hairer, E., (2011), Linear energy-preserving integrators for poisson systems, BIT Numerical Mathematics, 51, 91-101.
[7] M. Dahlby, M., and Owren, B., (2011) A general framework for deriving integral preserving numerical methods for PDEs. SIAM J. Sci. Comput., 33, 2318–2340.
[8] Frank,J., Moore, B.E., and Reich, S., (2006), Linear PDEs and numerical methods that preserve a multisymplectic conservation law. SIAM J. Sci. Comput., 28, 260–277.
[9] Ergenç, T. and Karasözen, B., (2006), Poisson integrators for Volterra lattice equations, Applied Numerical Mathematics, 56, 879-887.
[10] Hairer, E.,(2010), Energy-preserving variant of collocation methods, J. Numer. Anal. Ind. Appl. Math., 5, 73-84.
[11] Ito, M., (1980), An extension of nonlinear evolution equations of the K-dV (mK-dV) type to higher orders, J. Phys. Soc. Japan, 49, 771-778.
[12] Karasözen, B., (2004), Poisson integrators, Math. Comput. Modelling, 40, 1225-1244.
[13] Liu, Q. P., (2000), Hamiltonian structures for Ito's equation, Phys. Lett. A, 277, 31-34.
[14] Magri,F., (1998), A short introduction to Hamiltonian PDEs, Mat. Contemp., 15, 213-230.
[15] McLachlan, R. I., (2003), Spatial discretization of partial differential equations with integrals, IMA J. Numer. Anal., 23, 645-664.
[16] Olver, P.,(1995), Applications of Lie Groups to Differential Equations, Springer.
[17] Olver, P. J. and Rosenau, P., (1996), Tri-Hamiltonian duality between solitons and solutions having compact support, Phys. Rev. E, 53 (3), 1900-1906.
[18] G. R. W. Quispel and D. I. McLaren. A new class of energy-preserving numerical integration methods. J. Phys. A, 41:045206, 7, 2008.
[19] Schober, C.M., and Wlodarczyk, T.H., (2008), Dispersive properties of multisymplectic integrators. J. Comput. Phys., 227, 5090–5104.
[20] Schober, C.M. and Wlodarczyk, T.H., (2009), Dispersion, group velocity, and multisymplectic discretizations. Math. Comput. Simulation, 80, 741–751.
[21] Xu, Y. and Shu, C.-W., (2006), Local discontinuous Galerkin methods for the Kuramoto- Sivashinsky equations and the Ito-type coupled KdV equations, Comput. Methods Appl. Mech. Engrg., 195, 3430-3447.
[22] Zhao, P. F. and Qin, M. Z., (2000), Multisymplectic geometry and multisymplectic Preissmann scheme for the KdV equation, J. Phys. A, 33, 3613-3626.

Bülent Karasözen, for a photograph and biography, see TWMS Journal of Applied and Engineering Mathematics, Volume 1, No.2, 2011.

Görkem Şimşek, for a photograph and biography, see TWMS Journal of Applied and Engineering Mathematics, Volume 2, No.2, 2012.